J Therm Anal Calorim (2011) 103:257–265
DOI 10.1007/s10973-010-0967-6

Synthesis and structure of AMP/oxide support

V. Sydorchuk · S. Khalameida · J. Skubiszewska-Zięba · R. Leboda

Received: 12 March 2010 / Accepted: 9 July 2010 / Published online: 29 July 2010

Abstract Compositions based on oxides and containing 5–20% w/w of ammonium molybdophosphate have been synthesized by means of different routes. Prepared samples have been studied using nitrogen adsorption–desorption, XRD, DTA–TG, and FTIR spectroscopy. Keggin structure is retained at incorporation of ammonium molybdophosphate into siliceous framework or its deposition on oxide surface and duration following calcinations up to 500 °C. Compositions possess porous structure from micromesoporous to mesomacroporous depending on the preparation method.

Keywords Ammonium molybdophosphate · Sol–gel method · Milling · Fumed oxides · Micromesoporous and mesomacroporous structure

Introduction

Hetepolycompounds (HPCs) (polyoxometallates) in particularly heteropolyacids (HPAs) possess combination of attractive properties and advantages owing to their unique Keggin structure. Thus, HPAs contain exceptionally mobile protons, resulting in their high acidity and conductivity and utilization as promising acid catalysts, ion exchangers, and solid electrolytes [1–4]. Besides, transition metals with variable valency (V, Mo, and W) are part of the HPCs. Therefore, these compounds are perspective as oxidation catalysts [3–5], electro- and photochromic species [6, 7], photocatalysts [2, 3, 8, 9]. In other words, HPCs are versatile materials and have potential for numerous technological applications.

However, specific surface area of HPCs is very low, as a rule, which results in few active sites on their surface. Therefore, HPCs need granulation for effective utilization in adsorption columns and catalytic reactors. Besides, HPAs are hygroscopic, well soluble in water and oxygen-containing organic solvents, and chemically unstable for many practical purposes. Hence, deposition of HPCs on surface or incorporation in structure supports, first of all silica, is required [3, 4, 7, 10]. This is a proper way to stabilize HPCs. At the same time, minimal deterioration of useful properties of HPCs and their accessibility for substrates must be insured. Preliminary modification of surface by amino-groups permits to facilitate anchoring of HPAs to silica matrices. This route of HPCs grafting to the surface of support is the most popular [3, 7, 10, 11]. Similar procedures are also used for embedding of HPCs into oxide framework during sol–gel synthesis [3, 7, 12, 13]. In the latter case, incorporated moieties can possess singular physical, chemical, catalytic properties owing to achievement of nanodispersed state and restrictive influence of pore walls on enlargement of particles (confinement effect) [14, 15]. It should be noted that deposited or incorporated HPCs have improved properties in comparison with bulk HPCs in all the above mentioned cases of their application.

At the same time, described approaches which are used for deposition (incorporation) of HPCs on supports have

V. Sydorchuk (✉) · S. Khalameida
Institute for Sorption and Problems of Endoecology, NAS of Ukraine, Kyiv, Ukraine
e-mail: bilychi@ukr.net

V. Sydorchuk
O. O. Chuiko Institute of Surface Chemistry, NAS of Ukraine, Kyiv, Ukraine

J. Skubiszewska-Zięba · R. Leboda
Faculty of Chemistry, Maria Curie-Skłodowska University, Poland, Lublin

several disadvantages. Thus, compositions prepared through deposition of HPAs on pure (unmodified) silica cannot be applied in liquid media at least in water and organic oxygen-containing solvents. Meanwhile, their immobilization on activated surface drastically lowers acidity of deposited HPAs [3, 10]. Indicated limitations can be eliminated via utilization of insoluble salts of HPAs, for example, ammonium molybdophosphate (AMP). This compound itself is an effective ion exchange material, namely, adsorbent of cesium [4, 16–18] or catalyst of oxidation isobutene to methacrylic acid [5]. However, it possesses microcrystalline structure. Hence, from the practical point of view, granulation or deposition on ready-made granulated support is necessary for AMP. There are few studies devoted to employment of silica and alumina as support or binding material for granulation of AMP [19–23]. The authors of those studies have only described the adsorption properties and have not indicated structural characteristics of such compositions. Therefore, systematic investigations concerning this problem are absent.

The aim of this study is the synthesis of compositions AMP/oxide matrix using different methods based on modern approaches, namely, sol–gel incorporation and mechanochemical deposition, and study of structure of prepared hybrid materials. It should be noted that both indicated techniques are recently used for production of similar composites [3, 7, 12, 13, 24], but samples of the system AMP/oxide have not been earlier prepared via these methods.

Experimental

Reagents and materials

$(NH_4)_3PMo_{12}O_{40}\cdot 4H_2O$ (AMP) powder with specific surface area $S = 4$ m^2 g^{-1}, tetraethylorthosilicate (TEOS), acetic acid, ethyl alcohol (Fluka) were used in this study. All the reagents were analytical grade. Besides, fumed oxides—silica (aerosil A380), titania, and alumina (Oriana, Ukraine)—were utilized as supports. Oxides possess $S = 365$, 64, and 89 m^2 g^{-1}. Silica and alumina are X-ray amorphous, and titania is a mixture of anatase and rutile.

Samples preparation

Synthesis of compositions AMP/oxide containing 5–20% w/w of AMP was performed by two pathways.

Pathway I—incorporation via sol–gel technique

This method was used for production of AMP/silica samples only. Other compositions on the basis of silica, for example, described in [25, 26] were similarly synthesized. First of all, silicasol was prepared by the way of acid hydrolysis of TEOS in aqueous-ethanol medium and polycondensation of hydrolysis products at 60–70 °C. The routine procedure was following: 20 mL of TEOS, 8 mL of ethanol, and 1 mL of acetic acid (catalyst of hydrolysis) were vigorously mixed with the help of magnetic stirrer for 10 min, 16 ml of water was added dropwise and agitation lasted 30 min; 2.4 g of AMP that was previously comminuted was added using dry milling (15 min at 100 rpm) and further comminuted for 5 min. The obtained sol was turned into gel either at 25 °C on air for 15 min or underwent hydrothermal treatment in autoclave for 3 h. Both AMP-containing gels were washed from acetic acid by 1 L of water through decantation and dried on air at 25 °C for 72 h. Prepared dried xerogels were subjected to thermal treatment on air at 300, 400, 480, and 550 °C.

Pathway II—mechanochemical deposition

Compositions with the same ratio of constituent elements were prepared via milling of mixtures of AMP with fumed oxides at 200 and 400 rpm for 30 min. Air and water were media of mechanochemical process during dry and wet milling, respectively. Mechanochemical treatment (milling) was carried out in planetary ball mill Pulverisette 7, Premium line (Fritsch Gmbh). The amount of milled solid reagents was equal to 5 g. The amount of water added at wet milling was 40 mL. twenty-five balls of silicon nitride with diameter of 10 mm and total weight of 40.5 g and the vessel of silicon nitride volume of 80 mL were used.

Physical–chemical characterization

The parameters of porous structure were determined from isotherms of low-temperature nitrogen adsorption obtained with the help of analyzer ASAP 2405N (“Micromeritics Instrument Corp”). Outgassing temperature and duration were 150 °C and 2 h, respectively. Specific surface area S was calculated using the BET method. Volume of micropores V_{mi} was determined using t-method, and volume of mesopores V_{me} was calculated through BJH method. Sorption pore volume V_s consisting of V_{mi} and V_{me} was evaluated at relative pressure of nitrogen of about 1. Total pore volume V_Σ, which includes volume of micro-, meso-, and macropores, was determined via impregnation of samples dried at 150 °C with liquid water. Curves of pore size distribution (PSD) were constructed from the data desorption branch of the isotherms.

Crystal structure of prepared samples was examined on diffractometer HZG-4 Carl Zeiss, Jena (Cu Kα—radiation). Thermogravimetric analysis was carried out using Derivatograph-C (MOM, Budapest) in air with the heating rate

10°/min in the temperature range 20–800 °C (sample weight—30 mg). The FTIR spectra in the range 4000–450 cm^{-1} were registered using Perkin–Elmer spectrometer "Spectrum—One" (pellets with KBr with the mass ratio sample/KBr = 1:20).

Results and discussion

Sol–gel synthesis

The formation of uniform hydrogels and xerogels containing 5, 10, and 20% w/w of AMP and possessing developed porous structure is a result of realization of sol–gel process. It is interesting that 5% w/w adding of AMP causes significant increase of both specific surface area S (nearly 1.5 times) and total pore volume V_Σ (about 2 times) of composition in comparison with pure silicagel prepared in the same conditions (Table 1). Obviously, AMP moiety prevents strong compression of silica framework during the drying of hydrogel. As a result, sample with more accessible internal surface is formed. Introduction of 10% w/w of AMP leads to lesser growth of S and V_Σ, and addition of 20% w/w of AMP results in some lowering of S (in 1.2 times), while V_Σ approximately equals the value measured for pure silicagel. It is possible that larger admix of nonporous component (AMP) blocks some pores (first of all, micropores, which can be seen from Table 1) causing reduction of S and V_Σ. Micropore volume V_{mi} for all the three mixed samples is lesser than that for silicagel, but this parameter monotonically increases with increment of AMP content in composition, whereas V_{me} and V_Σ, on the contrary, diminish. Preliminary hydrothermal treatment of wet silica hydrogel and hydrogel containing 20% w/w of AMP promotes significant increase of S and V_Σ of resulted dried xerogels (it seems that accessibility of pores for adsorbate molecules increases). In second case, pore volume V_Σ reaches 0.54 $cm^3\ g^{-1}$, micropore volume—0.06 $cm^3\ g^{-1}$. It should also be noted that values of V_s and V_Σ of all the AMP/SiO_2 samples synthesized via sol–gel procedure are practically the same. The latter indicates the absence of macropores in these samples.

Described changes of porosity parameters, observed owing to embedding of AMP in siliceous framework, can be seen from the shape of corresponding nitrogen adsorption–desorption isotherms. Thus, isotherm obtained for pure silicagel, which relates to type I according to IUPAC classification (Fig. 1, curve 1), turns into isotherms of type IV with capillary-condensation hysteresis loop for AMP-containing samples (curves 2–4). This hysteresis loop of type H2 is located in wide region of relative pressure p/p_0 of adsorbate (nitrogen): 0.35–0.80. Meantime, curves of PSD for these samples are narrower and sharper (Fig. 1, curves 2–4) in comparison with that obtained for initial silica (curve 1). Therefore, samples containing AMP possess more uniform porous structure than that for pure silicagel. At the same time, the most probable pore diameter d which corresponds to maximum on PSD curves changes a little with increase of AMP content: from 2.6 nm for silicagel to 2.9–3.4 nm for compositions containing 5–20 w/w% of AMP. Therefore, mainly mesoporous samples of compositions are formed. These samples retain the initial values of parameters of porosity, including micropores volume, up to 480 °C during the following calcinations (Table 1, sample 8, Fig. 1, curve 4). This is an unexpected result since initial silica underwent partial sintering in the same conditions which is accompanied by noticeable lowering of both S and V_Σ.

Mechanochemical deposition

It is noteworthy that the compositions prepared during dry mechanochemical deposition of AMP on the fumed oxides (200–400 rpm, 0.5 h) are nonporous powders. It is not surprising, since the initial components are also nonporous,

Table 1 Parameters of porous structure of samples prepared via sol–gel route (pathway I)

No.	Samples	$S/m^2\ g^{-1}$	$V_s/cm^3\ g^{-1}$	$V_{mi}/cm^3\ g^{-1}$	$V_{me}/cm^3\ g^{-1}$	$V_\Sigma/cm^3\ g^{-1}$	d/nm
1	SiO_2 initial, 20 °C	642	0.30	0.22	0.08	0.30	2.6
2	SiO_2 initial, 150 °C	867	0.45	0.13	0.33	0.46	3.0
3	5% AMP/SiO_2, 20 °C	921	0.56	0.05	0.50	0.55	3.2
4	5% AMP/SiO_2, 150 °C	765	0.43	0.09	0.33	0.42	2.9
5	10% AMP/SiO_2, 20 °C	821	0.46	0.08	0.39	0.46	3.4
6	10% AMP/SiO_2, 150 °C	793	0.43	0.11	0.32	0.43	3.3
7	20% AMP/SiO_2, 20 °C	535	0.27	0.13	0.15	0.26	3.1
8	20% AMP/SiO_2 + TT480	825	0.54	0.06	0.46	0.54	3.1
9	20% AMP/SiO_2 + TT550	649	0.43	0.05	0.38	0.44	3.6
10	20% AMP/SiO_2, 150 °C	816	0.53	0.06	0.47	0.54	3.3

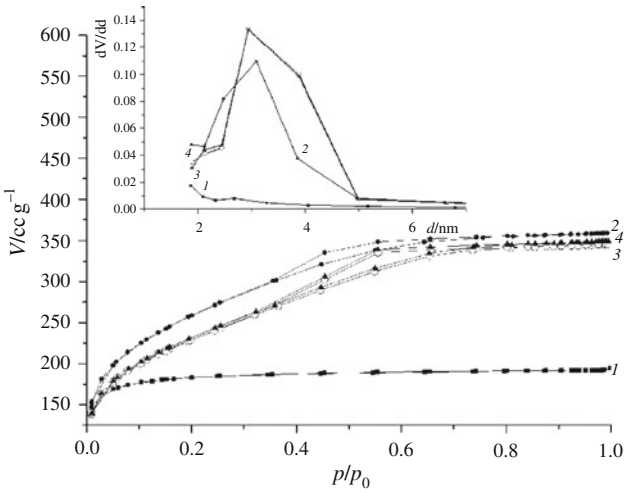

Fig. 1 Isotherms of nitrogen adsorption–desorption and pore size distribution (insert) for samples prepared via sol–gel method: SiO_2 bulk (*1*), and compositions containing 5% w/w AMP (*2*), 20% w/w AMP (*3*), and those calcined at 480 °C (*4*)

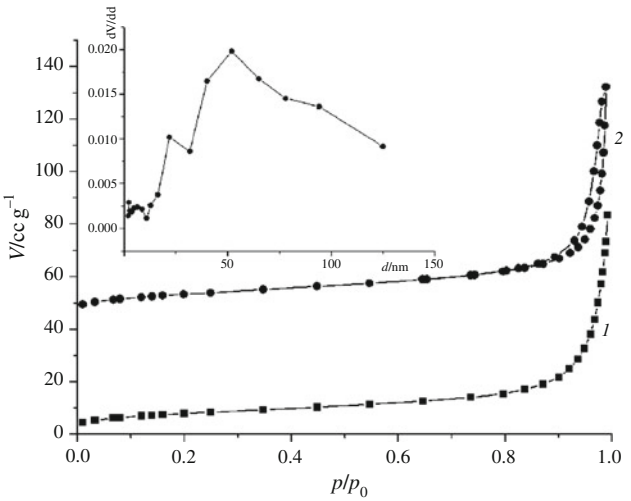

Fig. 2 Isotherms of nitrogen adsorption–desorption and pore size distribution (insert) for compositions based on titania containing 20% w/w AMP milled in air (*1*) and water (*2*) at 400 rpm

on the one hand, and the coalescence of particles of reagents in the porous skeleton in these conditions is unlikely, on the other hand. Indicated assumption was confirmed by the shape of nitrogen adsorption isotherms (without capillary-condensation hysteresis) obtained for the samples synthesized via dry milling: nitrogen adsorption isotherms relate to type II that is also characteristic for nonporous substance. Similar isotherms were obtained for the compositions on the basis of titania and alumina. An example of such isotherm is shown in Fig. 2 (curve 1). At the same time, specific surface area of all the resulted compositions monotonically reduces with increasing intensity of milling (rotation rate 200 and 400 rpm) compared with that of the initial supports. This can be seen from the Table 2 (samples 4, 6, 10, and 14). For samples milled at 400 rpm, the value of S decreases in 1.9–2.4 times. It should be noted that analogous milling of bulk AMP at 200 and 400 rpm promotes increase of its S from 4 to 8 and 11 $m^2\ g^{-1}$, respectively. These results agree with literature data: it is well known that specific surface area of nonporous substances diminishes, as a rule, during dry milling of superfine solids and increases when coarse powders are subjected to mechanochemical activation in a gaseous phase [27].

It is well known that nonporous superfine fumed oxides form structured gel-like dispersions (slurries) in water. Drying of these dispersions leads to the formation of porous xerogels. Similarly, mechanochemical deposition of AMP on silica surface (aerosil A380) in aqueous medium at 200 rpm results in formation of meso–macroporous structure with total pore volume $V_\Sigma = 1.35\ cm^3\ g^{-1}$ and mesopores volume $V_{me} = 0.85\ cm^3 \cdot g^{-1}$. Micropores in this deposited sample absent the volume of macropores V_{ma} is $0.5\ cm^3\ g^{-1}$. However, S for resulted composition is approximately equal to that for sample milled on air at 200 rpm. Increase of milling intensity in water to 400 rpm leads to sharp lowering of porosity (V_Σ) and some growth of S value. Meantime, the values of V_Σ and V_s coincide, which evidences the absence of macropores in this sample. Isotherms of type IV with hysteresis loop of H1 type that is located in the range of $p/p_0 = 0.75$–0.95 were obtained for compositions synthesized through wet milling (Fig. 3). Similar isotherms were presented by the authors [28] for deposited samples prepared by impregnation of fumed silica with aqueous solution of $H_3PMo_{12}O_{40}$. Besides, noticeable shift of the most probable pore diameter on PSD curves in region of lesser values is observed: from 40.4 nm for unmilled composition (sample 2) to 32.1 and 30.1 nm for samples milled in water under 200 and 400 rpm correspondingly. Therefore, more intensive milling results in denser packing of silica particles in framework in comparison with initial sample and sample prepared at 200 rpm. Uniform mesoporous structure without micro- and macropores is formed as a result.

Analogously to compositions obtained from A380, milled deposited sample based on alumina is homogeneously mesoporous. Moreover, its specific surface area, total pore volume (and volume of mesopores), and diameter of the mesopores determined from PSD curve are lesser compared with unmilled composition (samples 12, 13 from Table 2). The values of S, V_Σ and d are reduced, apparently due to greater compaction of particles composing the network of the gel in the process of milling. On contrary, compositions prepared via dispersion of AMP and titania in water (unmilled sample 8 in Table 2) and subsequent wet milling at 400 rpm (sample 9) contain macropores along with mesopores. Hence, in this case, the

Table 2 Parameters of porous structure of samples deposited on A380

No.	Samples	S/m^2 g^{-1}	V_s/cm^3 g^{-1}	V_{mi}/cm^3 g^{-1}	V_{me}/cm^3 g^{-1}	V_Σ/cm^3 g^{-1}	d/nm
1	A380 + H_2O	356	1.45	0.01	1.45	1.45	17.5
2	20% AMP + A380 + H_2O	272	1.41	–	1.40	1.76	40.4
3	20% AMP/SiO_2 200 rpm H_2O	199	0.84	0.01	0.85	1.35	32.1
4	20% AMP/SiO_2 200 rpm air	207	–	–	–	–	–
5	20% AMP/SiO_2 400 rpm H_2O	226	0.73	0.01	0.74	0.72	30.1
6	20% AMP/SiO_2 400 rpm air	181	–	–	–	–	–
7	TiO_2 + H_2O	61	0.43	–	0.42	0.54	35.4
8	20% AMP + TiO_2 + H_2O	48	0.32	–	0.33	0.59	56.3
9	20% AMP/TiO_2 400 rpm H_2O	30	0.11	–	0.11	0.41	52.0
10	20% AMP/TiO_2 400 rpm air	27	–	–	–	–	–
11	Al_2O_3 + H_2O initial	81	0.40	–	0.40	0.41	20.2
12	20% AMP + Al_2O_3 + H_2O	69	0.68	0.01	0.69	0.71	41.1
13	20% AMP/Al_2O_3 400 rpm H_2O	56	0.51	0.01	0.50	0.50	33.1
14	20% AMP/Al_2O_3 400 rpm air	47	–	–	–	–	–

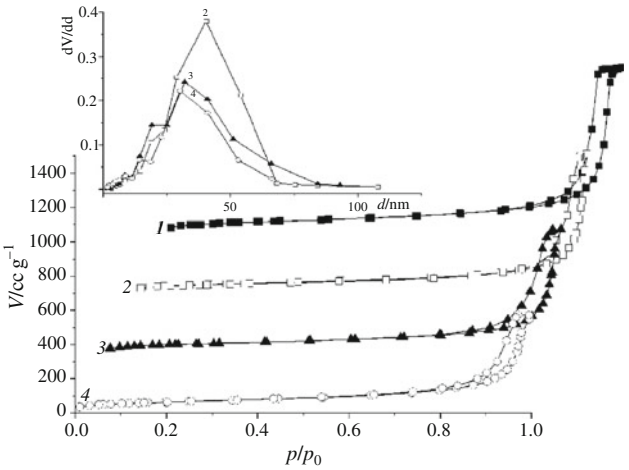

Fig. 3 Isotherms of nitrogen adsorption–desorption and pore size distribution (insert) for initial aerosilogel (*1*), and compositions based on A380 containing 20% w/w AMP: initial (*2*), and milled in water at 200 rpm (*3*), 400 rpm (*4*)

particles in the network are compacted to a lesser extent. However, mesoporous part is sufficiently uniform. Thus, adsorption–desorption isotherms of nitrogen obtained for milled sample have narrow hysteresis loop of type H1 located within $p/p_0 = 0.90$–0.99 (Fig. 2, curve 2). At the same time, pore diameter for this sample calculated from PSD corresponds to the upper limit of mesoporosity according to IUPAC classification, namely, equals 52.0 nm.

Different behaviors of the studied compositions during milling may be explained by the fact that the dispersions on the basis of amorphous silica and alumina are more plastic than that based on the crystal titania. Besides, silica and alumina possess larger specific surface area.

It should be noted that samples of the same composition but different porosity were synthesized through sol–gel and mechanochemical methods. This is illustrated by the compositions on the basis of silica. Obviously, the prepared samples have also mesopores of different shapes, which is evidenced by the different types of hysteresis loop for adsorption–desorption isotherms, as mentioned above. In other words, opposite ways of porous solid preparation, namely, condensation and construction were realized [29]. In first case, sufficiently coarse dispersed AMP embeds into structure when siliceous framework arises owing to hydrolysis-polycondensation of TEOS. Incorporated moiety, on the one hand, restricts mass transfer and, as a result, promotes formation of smaller silica globules possessing higher specific surface area, and, on the other hand, decreases shrinkage of gel during its drying. Consequently, micro–mesoporous samples with prevalence of mesopores (in comparison with pure silicagel) are formed.

At the same time, construction of porous framework from prefabricated siliceous globules occurs during milling of fumed silica in aqueous medium (with or without AMP). Specific surface area of dried xerogel is evaluated mainly by the globules size of globules, and the porosity depends on the density of their packing. The latter is determined by conditions of milling, first of all, by its intensity. Therefore, treatment at 200 rpm results in creation of meso–macroporous structure, and more vigorous milling leads to formation of homogeneous mesoporous xerogels. Since globule size in this case is larger, samples AMP/SiO_2 prepared from fumed silica are more large-porous in comparison with samples produced via sol–gel technique. At the same time, solely under dry milling, aggregation of silica and AMP particles without porosity formation is observed [30].

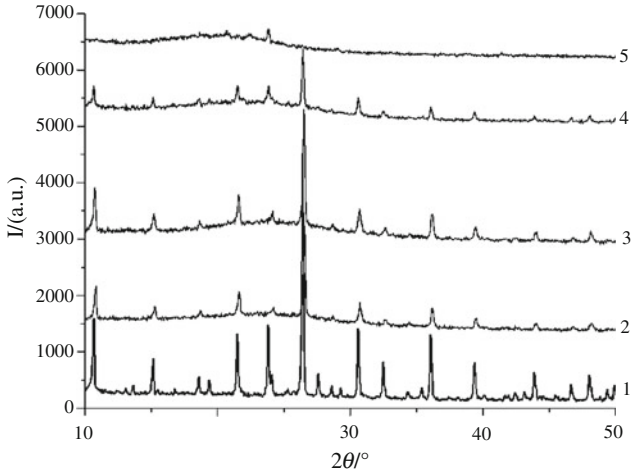

Fig. 4 Diffractograms of bulk AMP (*1*), and composition containing 20% w/w AMP prepared via sol–gel method: initial (*2*), and those calcined at 300 °C (*3*), 480 °C (*4*), 550 °C (*5*)

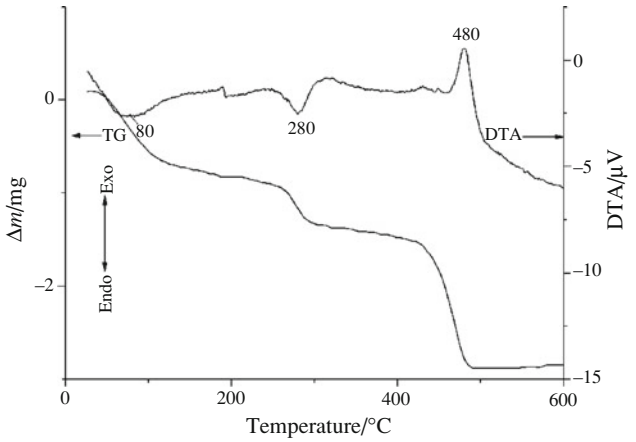

Fig. 5 Curves of DTA–TG for bulk AMP

XRD investigations

The XRD patterns of the crystalline AMP phase (JCPDS 09–0412) in the composition prepared through pathway I have been already presented, for the content of AMP 5% w/w. Its sufficiently intensive reflexes reveal in range of halo, characteristic for amorphous silica, at $2\theta = 10.7°$, 15.1°, 21.5°, 23.75°, and 26.45° (diffractogram is not presented). Increase of AMP content causes growth of intensities of all the reflexes corresponding to AMP, on the one hand, and practical complete disappearance of indicated halo, on the other hand (Fig. 4, diffractogram 2). The size of AMP crystallites calculated from the broadening of the most intense reflection ($2\theta = 26.45°$) on the Scherrer's equation gradually diminishes with increasing the APM content in the composition: from 31.0 nm for bulk AMP up to 24.1 nm for the sample containing 20% w/w of APM. Similar diffractograms with the same intensities of reflexes were also registered for the samples synthesized on the surface of fumed oxides via milling in air and water (these diffractograms are not presented). The size of AMP crystallites deposited on the silica surface is equal to 25.0 and 21.6 nm as a result of milling at 400 rpm in water and air, respectively. Their size in the compositions AMP/alumina is 22.4 and 18.1 nm. A similar calculation for compositions AMP/titania is difficult to make due to an overlapping of reflections of AMP and anatase.

Thermogravimetric analysis

Thermostability of prepared compositions was examined with the help of thermogravimetric analysis. It is known that HPCs contain two types of water, namely, crystallization and constitutional [3, 28, 31–33]. Curves of DTA and TG of bulk AMP used in our investigation are presented on Fig. 5. One can see that elimination of four molecules of crystallization water occurs in the range of temperature 20–310 °C. Two endoeffects with maxima at 80 °C and 280 °C reveal on DTA curve. Two molecules of water are removed during each step. In addition, 1.5 molecules of constitutional water (proton of ammonium group bound to the oxygen of the polyanion) and 3 molecules of ammonia are released at 400–500 °C. Thus, overlapping of several processes takes place in this temperature interval. There is near exoeffect with maximum around 480 °C and corresponding mass loss, which relates to thermolysis of AMP. Similar curves DTA–TG are shown in [22]. Total experimental mass loss at 20–500 °C reaches to 8.6% w/w, while theoretical value equals 7.7% w/w. The observed excess of experimental values of mass loss over the theoretical can be explained by the presence of a small amount of adsorbed water on the surface of AMP.

More intensive endoeffects and, respectively, greater mass loss were displayed on DTA–TG curves of compositions prepared via sol–gel and mechanochemical method at 20–200 °C (Figs. 6, 7, and 8, correspondingly). This is obvious due to the fact that the porous AMP/oxide samples retain more of the adsorbed water compared with nonporous AMP bulk. It is interesting that intensity of effect, its temperature, and corresponding mass loss are higher for composition prepared through sol–gel way (135 °C) since this sample possesses narrower pores as mentioned above. However, the curves obtained for all the compositions are similar to those obtained for AMP bulk in the range of temperature up to 700 °C. They contain the same effects and stages of gases release. Additional effects caused by crystallization process of aluminum oxide are present on the DTA–TG curves obtained for the composition AMP/alumina (Fig. 8). It is noteworthy that exoeffect of ammonium salt destruction locates in temperature range 400–500 °C with maximum at 465–484 °C. The latter is confirmed by

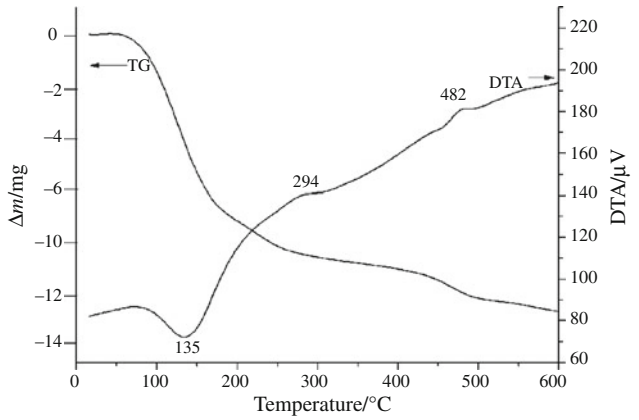

Fig. 6 Curves of DTA–TG for composition containing 20% w/w AMP prepared via sol–gel method

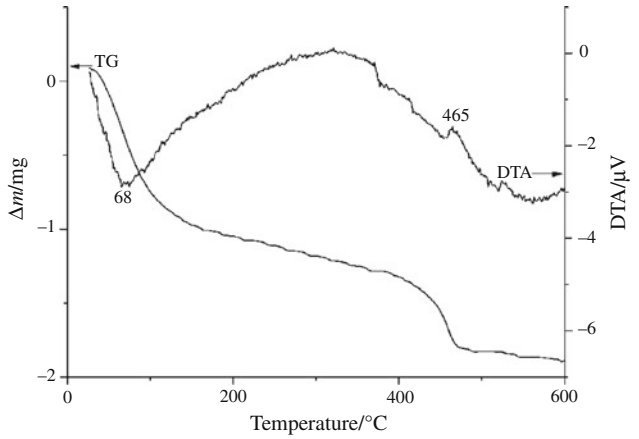

Fig. 7 Curves of DTA–TG for composition based on A380 containing 20% w/w AMP prepared via wet milling at 200 rpm

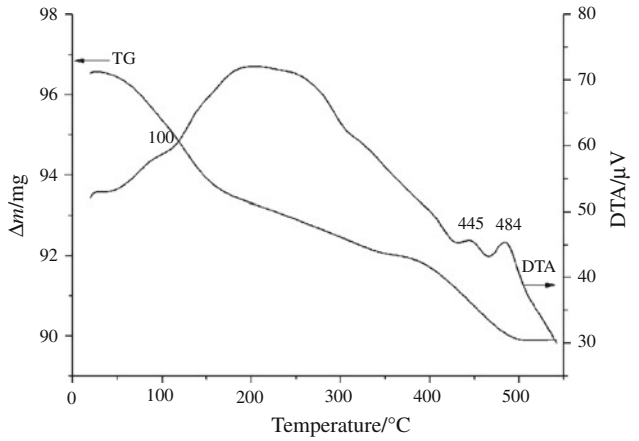

Fig. 8 Curves of DTA–TG for composition based on alumina containing 20% w/w AMP prepared via wet milling at 400 rpm

XRD findings. Samples calcined at 300–480 °C retain the crystalline structure of salt, whereas those annealed at 550 °C contain only poorly crystallized molybdenum trioxide (Fig. 4, diffractograms 2–4). Therefore, thermostability of both incorporated and deposited compositions and bulk AMP is the same, which is important for their application as heterogeneous catalysts in gas-phase processes. The latter does not agree with the results of some other studies. Thus, steadiness of deposited HPCs under heating can be decreased as authors [28, 33] have noted.

FTIR study

Additional data concerning of AMP/SiO_2 design and thermostability of Keggin structure were obtained by means of FTIR spectroscopy. The polyanion of molybdophosphorous acid shows four main specific absorption lines between 1200 and 700 cm^{-1} assigned to the stretching vibrations ν_{as} P–O, ν_{as} Mo = O, ν_{as} Mo–O_c–Mo, and ν_{as} Mo–O_e–Mo [3, 28, 34]. Spectra of samples prepared via different pathways are shown in Figs. 7, and 8. Following absorption bands (a.b.) were registered in this region for AMP bulk: 1060, 969, 865, and 803 cm^{-1} (Fig. 8, curve a). As a result of AMP embedding in framework or its deposition on surface of silica indicated, a.b. maintain their positions, but they are overlapped with strong a.b. of silica, namely, 1085, 950, and 800 cm^{-1}. Therefore, a.b. around 865 cm^{-1} and a.b. 1060 cm^{-1} (for compositions synthesized only through sol–gel procedure—Fig. 9) are satisfactorily resolved in this spectrum range whose presence and intensity can be clear evidence of Keggin unite preservation. Thus, intensity of a.b. around 865 cm^{-1} band somewhat increases owing to rise of AMP content in compositions prepared via sol–gel technique (Fig. 9, curves a–c). Intensity of band around 1407–1419 cm^{-1}, relating to vibrations of NH_4^+ group, is more sensitive to both the amount of AMP (Fig. 9, curves a–c) and the extent of its destruction during calcinations or

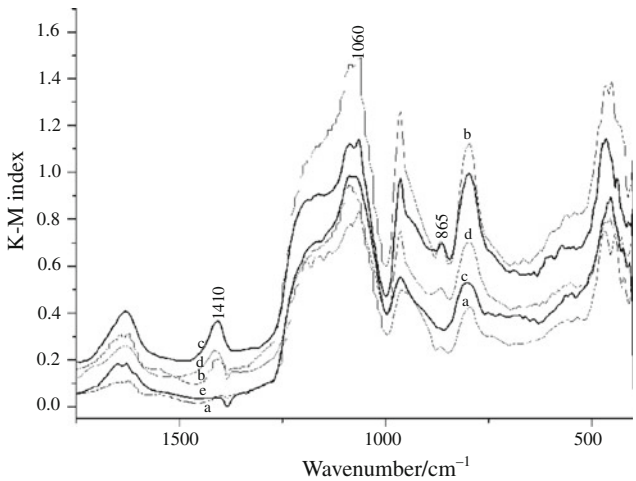

Fig. 9 FTIR spectra for compositions prepared via sol–gel method: containing 5% w/w AMP (**a**), 10% w/w AMP (**b**), 20% w/w AMP (**c**), and those calcined at 300 °C (**d**), 500 °C (**e**)

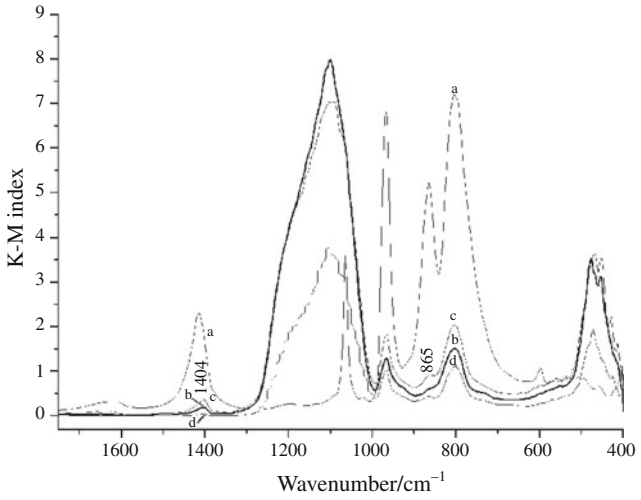

Fig. 10 FTIR spectra for bulk AMP (*a*), and compositions prepared via milling: at 200 rpm in air (*b*), in water (*c*), and at 400 rpm in air (*d*)

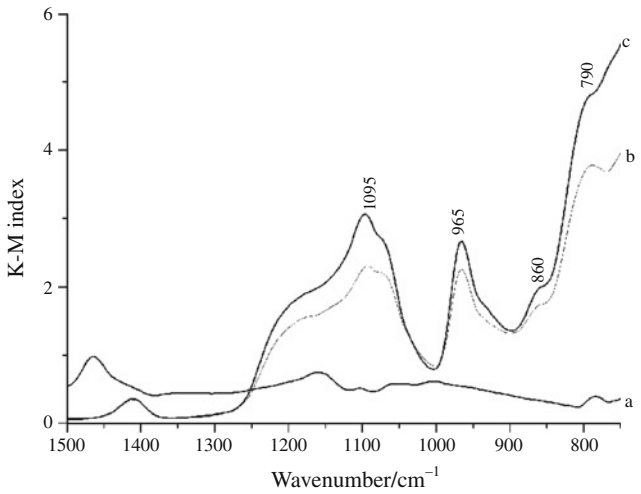

Fig. 11 FTIR spectra for bulk titania (*a*), and compositions based on titania prepared via milling: at 400 rpm in air (*b*), in water (*c*)

milling (Fig. 9, curves d, e and Fig. 10, curves b–d, respectively). Thus, intensity of this a.b. grows by nearly one order when AMP concentration in silica matrix rises from 5 to 20% w/w (Fig. 9, curves a–c). On the other hand, it gradually subsides in consequence of elevation of calcinations temperature of all the compositions and exhaustively disappears from spectra of samples annealed at 550 °C (as and a.b. 865 cm^{-1}) which one can see in Fig. 9 (curves d, e). Analogously, dry milling of both bulk AMP and its mixture with fumed silica results in partial decomposition of heteropolyanion structure (Fig. 10, curves a, b, and d), while wet milling practically does not destroy it (Fig. 10, curves c). Spectra obtained for the compositions based on titania and alumina also confirm maintaining the structure of AMP on support surface. This is most clearly revealed on the spectra of samples prepared on the basis of TiO_2. As titania absorbs weakly in the range 1100–700 cm^{-1} (Fig. 11, curve a), the absorption bands of AMP are well displayed (curves b, c). Therefore, FTIR spectra on the whole agree with data obtained using XRD and DTA–TG.

Conclusions

Therefore, first synthesis of compositions of ammonium molybdophosphate with silica, titania, and alumina, which consist of 5–20% w/w of AMP, is realized via sol–gel and mechanochemical techniques. All the samples containing crystalline AMP retain Keggin structure up to 500 °C, which is confirmed by XRD, DTA–TG, and FTIR data. Compositions prepared through sol–gel route possess micro–mesoporous structure. On the contrary, milled samples are meso–macroporous. At the same time, porosity of all the compositions is also thermostable up to 500 °C.

Acknowledgements This study was supported by International Visegrad Fund (Contract No. 50910373).

References

1. Pope MT. Heteropoly and isopoly oxometallates. Berlin: Springer; 1983.
2. Pope MT, Müller A. Polyoxometalate chemistry: an old field with new dimensions in several disciplines. Angew Chem Int Ed Engl. 1991;30:34–48.
3. Okuhara T, Mizuno N, Misono M. Catalytic chemistry of heteropoly compounds. Adv Catal. 1996;41:113–252.
4. Moffat JB. The surface and catalytic properties of heteropoly oxometalates, fundamental and applied catalysis. New York: Kluwer Academic/Plenum Publishers; 2001.
5. Cavani F, Mezzogori R, Pigamo A, Trifiro F, Etienne E. Main aspect of the selective oxidation of isobutene to methacrylic acid catalyzed by Keggin-type polyoxometallates. Catal Today. 2001;71:97–110.
6. Yamaze T. Photo- and electrochromism of polyoxometalates and related materials. Chem Rev. 1998;98:307–26.
7. Zhang TR, Feng W, Lu R, Bao CY, Li TJ, Zhao YY, Yao JN. Preparation of photochromic sol-gel composite films containing dodecaphosphotungstic acid. Mater Chem Phys. 2002;78:380–4.
8. Kormali P, Troupis A, Triantis T, Hiskia A, Papaconstantinou E. Photocatalysis by polyoxometallates and TiO_2: a comparative study. Catal Today. 2007;124:149–55.
9. María D, Hernández-Alonso A, Fernando Fresno B, Silvia Suárez A, Juan M. Coronado development of alternative photocatalysts to TiO_2: challenges and opportunities. Energy Environ Sci. 2009;2:1231–57.
10. Sydorchuk V, Zazhigalov V, Khalameida S, Skubiszewska-Zięba J, Charmas B, Leboda R. Deposition of tungsten heteropoly-compounds on activated silica surface. Colloids Surf A. 2009; 341:53–9.
11. Tarlani A, Abedini M, Nemati A, Khabaz M, Amini MM. Immobilization of Keggin and Preyssler tungsten heteropolyacids on various functionalized silica. J Colloid Interface Sci. 2006; 303:32–8.

12. Mrowiec-Bialon J, Turek W, Jarzębski AB. Preparation of highly active heteropolyacid-silica composite catalysts using sol–gel method. React Kinet Catal Lett. 2002;76:213–9.
13. Fuchs V, Mendez L, Blanco M, Pizzio L. Mesoporous titania directly modified with tungstophosphoric acid: synthesis, characterization and catalytic evaluation. Appl Catal A. 2009; 358:73–8.
14. Alcoutlabi M, McKenna GB. Effect of confinement on material behaviour at the nanometer size scale. J Phys Condens Matter. 2005;17:R461–524.
15. Burt MC, Dave BC. Externaly dynamic confinement effect in organosilica sol-gels. J Am Chem Soc. 2006;128:11750–1.
16. Amphlett CB. Inorganic ion exchangers. New York: Elsevier; 1964.
17. Clearfield A. Inorganic ion exchanger materials. Boca Raton: CRC Press; 1982.
18. Smit J. Insoluble heterolyacid salts. In: Qureshi M, Varshney KG, editors. Inorganic ion exchangers in chemical analysis. Boston: CRC Press; 1991. p. 68–9.
19. Caletka R, Konečnỳ C. Adsorption properties of ammonium molybdophosphate supported in pores of silica gel. Radiochim Radioanal Lett. 1972;12:325–9.
20. Doležal J, Stejskal J, Tympl M, Kouřím V. Improved inorganic ion-exchangers. II Ammonium molybdophosphate–silica gel system. J Radioanal Chem. 1974;21:381–7.
21. Terada K, Hayakawa H, Sawada K, Kiba T. Silica gel as a support for inorganic ion-exchangers for the determination of cesium-137 in natural waters. Talanta. 1970;17:955–63.
22. Tranter TJ, Aloy AS, Sapozhnikova NV, Knecht DA, Todd TA. Porous crystalline silica (gubka) as a inorganic support matrix for novel sorbent. Mat Res Soc Symp. 2002;713: JJ11.68.1–7.
23. Satyannarayana J, Murthy GS, Sassidhar P. Adsorption studies of cesium on a new inorganic exchanger ammonium molybdophosphate–alumina (AMP–Al2O3). J Radioanal Nucl Chem. 1999;242:11–6.
24. Matsuda A, Daiko Y, Ishida T, Tadanaga K, Tatsumisago M. Characterization of proton-conducyive SiO2–H3PMo12O40 composites prepared by mechanochemical treatment. Solid State Ion. 2007;178:709–12.
25. Berezovska IS, Yanishpolskii VV, Tertykh VA. Synthesis of mesoporous silicas inside large pores of inorganic matrix. J Therm Anal Calorim. 2008;94:649–53.
26. Sidorchuk VV, Tertykh VA, Klimenko VP, Ragulya AV. Formation and some properties of barium titanate embedded into porous matrices. J Therm Anal Calorim. DOI 10.1007?s 10973-010-0814-9.
27. Heinike G. Tribochemistry. Berlin: Academie Verlag; 1980.
28. Popa A, Sasca V, Stefanescu M, Kiš EE, Marinković-Nedučin R. The influence of the nature and textural properties of different supports on the thermal behavior of Keggin type heteropolyacids. J Serb Chem Soc. 2006;71:235–49.
29. Iler RK. Chemistry of silica. New York: Wiley; 1979.
30. Sydorchuk V, Khalameida S, Zazhigalov V, Skubiszewska-Zięba J, Leboda R, WieczorekCiurowa K. Influence of mechanochemical activation in various media on structure of porous and nonporous silicas. Appl Surf Sci. (in press).
31. Sasca V, Ştefănescu M, Popa A. Studies on the non-isothermal decomposition of $H_3PMo_{12}O_{40}{\cdot}xH_2O$ and $H_4PVMo_{11}O_{40}{\cdot}yH_2O$. J Therm Anal Calorim. 1999;56:569–78.
32. Sasca V, Stefanescu M, Popa A. Thermal behavior of the polyoxometalates derived from $H_3PMo_{12}O_{40}$ and $H_4PVMo_{11}O_{40}$. J Therm Anal Calorim. 2003;72:311–22.
33. Rocchiccioli-Deltcheff C, Amirouche M, Herve G, Fournier M, Che M, Tatibouet JM. Structure and catalytic properties of silica-supported polyoxomolybdates: II. Thermal behavior of unsupported and silica-supported 12-molybdosilicic acid catalysts from IR and catalytic reactivity studies. J Catal. 1990;126:591–9.
34. Bridgeman AJ. Density functional study of the vibrational frequencies of a Keggin-heteropolyanions. Chem Phys. 2003;287: 55–69.